Anti-Cancer Drugs 1997, 8, pp. 164–173

Enhancement of etoposide (VP-16) cytotoxicity by enzymatic and photodynamically induced oxidative stress

Tsvetan G Gantchev and Darel J Hunting
MRC Group in the Radiation Sciences, Department of Nuclear Medicine and Radiobiology, Faculty of Medicine, University of Sherbrooke, Sherbrooke, Quebec J1H 5N4, Canada. Tel: (+1) 819 564-6501; Fax: (+1) 819 564-5442.

The effects of glutathione (GSH) depletion by buthionine sulfoximane (BSO) or by photosensitization-induced oxidative stress using metallo-phthalocyanines ($MePcS_4$) on etoposide (VP-16) cytotoxicity against K562 human leukemic cells were investigated. Both treatments enhanced VP-16 toxicity in a markedly synergistic way, as revealed by combination index analysis procedure. Synergistic drug interactions were accompanied by a supra-additive induction of DNA strand breaks. The proposed role of intracellular GSH in preventing metabolic transformations of VP-16 and thus decreasing its toxicity was confirmed by electron spin resonance (ESR) monitoring of the accumulation of the VP-16 phenoxyl radical in cell cytoplasm subjected to GSH depletion. Taken together the results emphasize the beneficial effect of GSH-related oxidative stress in enhancement of etoposide toxicity and possibly in its anticancer applications.

Key words: Cytotoxicity, etoposide, glutathione, photosensitization, synergism, VP-16.

Introduction

Etoposide (VP-16), a semi-synthetic derivative of podophyllotoxin, has been used in treating various malignancies, including small cell bronchogenic carcinoma, lymphomas, leukemias, bladder cancer and ovarian cancer. It has been successfully used in combination with cisplatin, cyclophosphamide, doxorubicin and vincristin. The mechanisms of cytotoxicity of VP-16 have been shown to involve trapping of the topoisomerase II–DNA cleavable complex[1] and/or induction of direct DNA breaks.[2,3] Since etoposide itself does not damage purified DNA[4] it has been suggested that the direct formation of DNA breaks by etoposide is a result of intracellular enzymatic metabolism of the drug, which involves transformations within its pendant demethoxyphenolic group.[5–7] In particular, some peroxidases, prostaglandin synthetase, tyrosinase and P450-dependent mono-oxygenases may be involved in the intracellular activation of VP-16.[8–10] Several metabolic products, such as the *ortho*-quinone[7] and the dihydroxy[11] derivatives of the drug, as well as the short-lived intermediates (phenoxyl and semiquinone free radicals) are involved in various chemical reactions that can damage DNA and other cell constituents.[7,12,13] Recent studies have also shown that the VP-16 phenoxyl radical, the primary free radical product formed during oxidative metabolism of the drug, can react with intracellular reductants (e.g. free and protein bound thiols, ascorbic acid, etc.) thus modulating the toxicity of the drug.[14–16] These interactions have been shown to prevent etoposide from undergoing further transformations, to reconvert the VP-16 to its original form,[14,17] and to cause accumulation of cytotoxic activated oxygen species.[18] Glutathione (GSH) is the main non-protein thiol involved in numerous cellular defences against activated oxygen species and other toxicants produced during exposure to therapeutic and environmental chemicals or ionizing radiation.[19,20] Etoposide in its original form does not react with GSH; however, some of its metabolites have this potential. It might be, therefore, anticipated that a change in GSH content could affect VP-16 cytotoxicity at several of the steps in its intracellular transformation.

Based on the above considerations, we have examined the relationship between the toxicity of VP-16 and cellular GSH levels modulated either enzymatically by inhibition of γ-glutamylcysteine synthetase using buthionine sulfoximine (BSO) or by oxidative stress induced by photosensitization with aluminum and zinc-metallo-phthalocyanines. BSO is an irreversible inhibitor of γ-glutamylcysteine synthetase which blocks *de novo* glutathione

This work has been supported by the Medical Research Council of Canada and Ministère de l'Enseignement Supérieur et de la Science du Gouvernement du Québec.

Correspondence to TG Gantchev

synthesis in cells and tissues, and is frequently used at non-toxic concentrations to deplete cells and tumors of GSH, to increase their sensitivity to drugs and radiation.[21]

Metallo-phthalocyanines (MePc) are photosensitizers under development as second-generation photodynamic agents to supplant Photofrin II, the drug currently used in the photodynamic therapy (PDT) of various malignancies. Recently, we have studied the cytotoxic effects of a combination of a water-soluble aluminum phthalocyanine tetrasulfonate ($AlPcS_4$) and VP-16 in K562 human leukemic cells.[22] Under certain experimental conditions there was a synergistic enhancement of cytotoxicity which was accompanied by other supra-additive effects on cells, including induction of supra-additive G_2/M cycle arrest and apoptosis, as determined by internucleosomal DNA fragmentation. In the latter study, however, the underlying biochemical mechanisms responsible for these synergistic drug interactions were not addressed.

We have, however, shown that photosensitization with $MePcS_4$ can effectively oxidize both free thiols and protein thiols, a process mediated by reactive oxygen species.[23] In view of these photodynamic properties of $MePcS_4$, we hypothesized that photosensitization-induced oxidative stress, and in particular a depletion of intracellular GSH, might be involved in the synergistic enhancement of etoposide toxicity.

In the present study, using the median effect/combination index analysis, we analyzed the synergistic enhancement of VP-16 cytotoxicity by BSO or by photosensitization in the presence of $AlPcS_4$ and $ZnPcS_4$. This synergistic cytotoxicity was paralleled by a supra-additive increase in the number of DNA strand breaks. Finally, in order to correlate the effect of the depletion of cytoplasmic GSH content with the effectiveness of VP-16 metabolic transformations, we measured the rate of *in vitro* accumulation of its phenoxyl radical intermediate in cytoplasmic preparations using electron spin resonance (ESR).

Materials and methods

Reagents

Etoposide (VP-16) was purchased from Sigma (St Louis, MO). The compound was dissolved in dimethyl sulfoxide (DMSO), aliquoted and stored at −20°C. Further dilutions were made in RPMI medium immediately before use. Aluminum and zinc tetrasulfonated metallo-phthalocyanines ($AlPcS_4$ and $ZnPcS_4$) were synthesized in the laboratory of Dr JE van Lier, purified by HPLC, dialyzed to homogeneity and dissolved in phosphate buffered saline (PBS) to yield stock solutions of 2.0 mM, as measured spectrophotometrically ($\varepsilon = 2.5 \times 10^4\ M^{-1}\,cm^{-1}$ in DMSO; at *Q*-band λ_{max}). Buthionine-[*S*,*R*]-sulfoximine (BSO), glutathione, GSH (reduced form), glutathione peroxidase (GSH-px, EC 1.11.1.9), tyrosinase (EC 1.14.18.1), glutathione reductase (EC 1.6.4.2), NADPH, 5,5′-dithio-bis(2-nitrobenzoic acid) (DTNB, Ellmans's reagent) were purchased from Sigma and used as supplied. Cumene hydroperoxide (CumOOH) and the sulfhydryl reagent, 2-vinylpyridine were obtained from Aldrich (WI, USA). [^{14}C]dThd and [^{3}H]dThd were purchased from New England Nuclear (Boston, MA). All other chemicals were of highest available purity.

Cell culture and drug treatment

Human chronic myelogenous leukemia cells, K562 (ATCC CCL 243), were grown in RPMI 1640 medium, supplemented with glutamine, 1 mM GSH, 10% FBS, 50 μg/ml gentamycin and 10 mM HEPES. All experiments were performed with exponentially growing (asynchronous) cells. Before experiments, the cells were seeded in 3:1 v/v parts fresh to conditioned medium. On the next day, cells were counted, the cell density was adjusted by addition of a small volume of fresh RPMI medium to give 5×10^5 cells/ml and cells were incubated with BSO or $MePcS_4$ (in dark). After pre-incubation with BSO for 4.5 h or with $MePcS_4$ for 4 h, after 24 h (or longer periods) the cells were washed once in PBS and once in RPMI medium (without FBS) and resuspended in complete RPMI medium (conditioned to fresh = 1:3 v/v). Thereafter, cells were exposed either to VP-16, photo-irradiation or a combination of the two. To avoid high toxic effects of VP-16 alone, the incubation time with the drug was diminished to 20 min (unless otherwise stated). When cells were to be subjected to both VP-16 and photodynamic treatment, they were pre-incubated in the dark and then photo-irradiated for a given time period so as to achieve the required light dose and a total incubation time with VP-16 of 20 min. Following treatment, all cell groups (controls and treated cells) were washed, resuspended in growth medium and kept for further analyses. Photosensitization was performed using broad spectrum IR-filtered red light ($\lambda > 580$ nm, $I = 10\ mW/cm^{-2}$). Cells (12 ml suspension) were irradiated in ventilated (green-cap) Falcon, 75 cm^2 plastic incubation flasks and were

gently shaken during light exposure. Dark incubation with $MePcS_4$ was virtually non-cytotoxic. Exposure of cells incubated with VP-16 to red light, in the absence of $MePcS_4$, did not alter VP-16 toxicity.

Cytotoxicity assessment and analytical procedures

Evaluation of drug toxicity was performed using a clonogenic assay. After treatment, cells were incubated in the dark for 4–5 h, counted, diluted in RPMI medium and plated in a standard fashion in soft (0.33%) agar in 35 mm Petri dishes (usually 300, 600 or 1200 cells per dish in triplicate). On the 15th day colonies were fixed with ethanol, stained with crystal violet and counted under an inverted microscope.

To analyze dose–effect relationships in the combination treatment of cells with VP-16 and BSO or $MePcS_4$ photosensitization, we selected the median-effect combination index algorithm, as described by Chou and Talalay.[24] We used the linearized median effect equation $\log[(f_u)^{-1} - 1] = m\log(D) - m\log(D_m)$, where $f_u = 1 - f_a$ is the fraction of cells non-responding to treatment and f_a is the fraction of cells affected by treatment, respectively; m is a coefficient determining the sigmoidality of the dose–effect curve, D is drug dose and $D_m = IC_{50}$ is the dose required to produce the median effect. The combination index (CI) was calculated at f_a levels along the interval from 0.05 to 1.0. By definition $CI < 1.0$ indicates synergistic, $CI = 1.0$ additive and $CI > 1.0$ antagonistic drug interactions. Based on our previous work, interactions between VP-16 and photosensitization are likely to fit a mutually non-exclusive drug interaction model, which in fact represents the most unfavorable condition to achieve synergism.[22]

Measurement of DNA strand breaks

DNA strand breaks were measured using a modified version of the alkaline elution method of Kohn *et al.*,[25] as described previously.[26] Approximately 2×10^6 cells, prelabeled with [^{14}C]dThd (15 nCi/ml for 16 h) were damaged and incubated as described, and then harvested by centrifugation and resuspended in 2 ml of ice-cold PBS containing 0.02% EDTA. Then 1 ml of cell suspension was added to 20 ml of ice-cold PBS containing an internal standard consisting of about 5×10^5 cells which had been labeled for about 16 h with 100 nCi/ml [^{3}H]dThd (1 μM) and irradiated with either 300 or 1000 rad of γ-radiation, depending on the required range of the assay. The cells were collected on a polycarbonate filter (Nucleopore, Pleasanton, CA), washed with 5 ml of PBS, lysed with 4 ml of 2 M NaCl, 40 mM EDTA, 0.2% *N*-laurylsarcosine, pH 10. This was followed by 5 ml of 20 mM EDTA, pH 10, and then the DNA was eluted with 20 mM EDTA adjusted to pH 12.0 with tetrapropylammonium hydroxide. The radioactivity of the eluted DNA was determined by liquid scintillation counting.

GSH determination

Levels of cytoplasmic GSH were determined by glutathione reductase-5,5′-dithio-bis(2-nitrobenzoic acid) using the spectrophotometric method of Tietz as modified by Griffith.[27] Cell cytoplasm was obtained following digitonin-induced membrane permeabilization and separation from the organellar content by centrifugation, as described previously.[23] Experiments performed using digitonin concentrations from 25 to 400 μg/ml did not change the total amount of measured glutathione, indicating that only cytoplasmic GSH was released by this treatment. Cell permeabilization with 100 μg/ml digitonin was used throughout this study.

ESR spectroscopy

Tyrosinase-catalyzed oxidation of VP-16 and detection of the generated VP-16 phenoxyl radical was monitored by ESR spectroscopy. The reaction was performed in a phosphate buffer (pH 7.4 at 22°C) or in cell cytoplasm using 5 U/μl tyrosinase and 600 μM VP-16 in a 200 μl quartz aqueous ESR cell. ESR spectra were recorded on an E9 Varian ESR spectrometer using: 334 mT center of the magnetic field, 4 mT scan sweep, 0.032 mT modulation amplitude and 15 mW microwave power. Kinetic measurements were performed using the same parameters except for using a zero scan sweep and increasing the modulation amplitude and receiver gain ×8.

Results

Toxicity of VP-16 and BSO

Treatment of K562 cells with BSO for 4.5 h at concentrations less than 60 μM followed by replace-

ment of cells in fresh medium had little effect on the clonogenic capacity of the cells (Figure 1). Higher concentrations, however, inhibited cell growth and reduced clonogenecity, with an IC_{50} of about 180 μM. When cells were co-incubated with a constant concentration of BSO (50 μM) for 4.5 h and variable concentrations of VP-16 for 20 min, a pronounced supra-additive cytotoxic effect was observed (Figure 1). To further evaluate the cellular responses following simultaneous drug treatment, we performed a combination index analysis based on the median effect principle.[24] The cells were exposed to different concentrations of VP-16 (20 min) and BSO (4.5 h), while maintaining a constant molar drug ratio: VP-16/BSO = 1/10. The combination index (CI) was calculated assuming both possible types of drug interactions: mutually exclusive and non-exclusive. The plots shown in Figure 2 indicate that both models predict synergistic drug interactions (CI < 1.0) for virtually all F_a, except in the case of non-exclusive interactions under severe cell treatment conditions ($F_a \sim 1.0$).

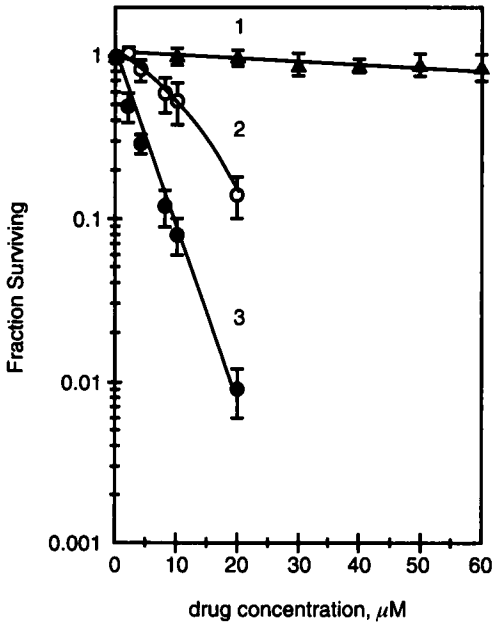

Figure 1. Clonogenic survival after exposure of K562 cells to different concentrations of: BSO for 4.5 h (1, ▲), VP-16 for 20 min (2, ○), and after combined treatment with BSO (50 μM, 4.5 h) and different concentrations of VP-16 for 20 min (3, ●). Average data from triplicate experiments.

Toxicity of VP-16 and photosensitization with $MePcS_4$

In the present study, we analyzed the effect of photodynamic treatment with $AlPcS_4$ and $ZnPcS_4$ on the toxicity of VP-16. In order to gain a deeper insight into the processes involved, we examined three variables (incubation time, drug ratio and light dose) which may influence the outcome of combination treatment. Figure 3(A) shows the results of the combination index analyses when short pre-illumination incubation times (4 h) with $MePcS_4$ were used, as [VP-16]/[$MePcS_4$] = 1/2. The drug interactions, as evaluated for a mutually non-exclusive process, are predominantly synergistic. The relatively weak antagonism obtained with $ZnPcS_4$ was attenuated when a higher light dose was used (curve 2 versus curve 3 in Figure 3A). In contrast, when photosensitizers were incubated with cells for longer times before light exposure (24 h or more), the combination treatment was markedly antagonistic and was synergistic only at $F_a > 0.45$ ($AlPcS_4$) and $F_a > 0.85$ ($ZnPcS_4$), even for lower relative concentrations of $AlPcS_4$ and $ZnPcS_4$ in the medium ([VP-16]/[$MePcS_4$] = 1/1) (Figure 3B). These antagonistic interactions are suggested to result from the higher photodynamic toxicity of $MePcS_4$ after longer pre-incubation with cells, associated with a different intracellular localization pattern of the photosensitizers (see Discussion).

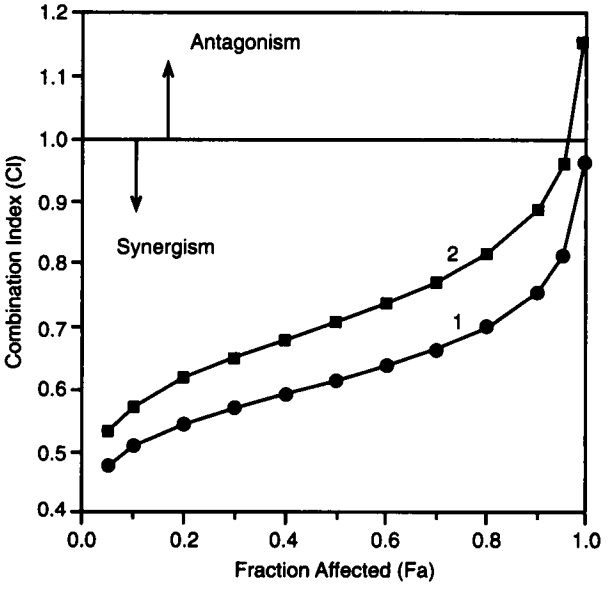

Figure 2. Plots of combination index (CI) versus fraction affected (F_a) for [VP-16]/[BSO] = 1/10. Data from clonogenic toxicity of the drugs and calculated for mutually exclusive (1, ●) and non-exclusive (2, ■) interactions.

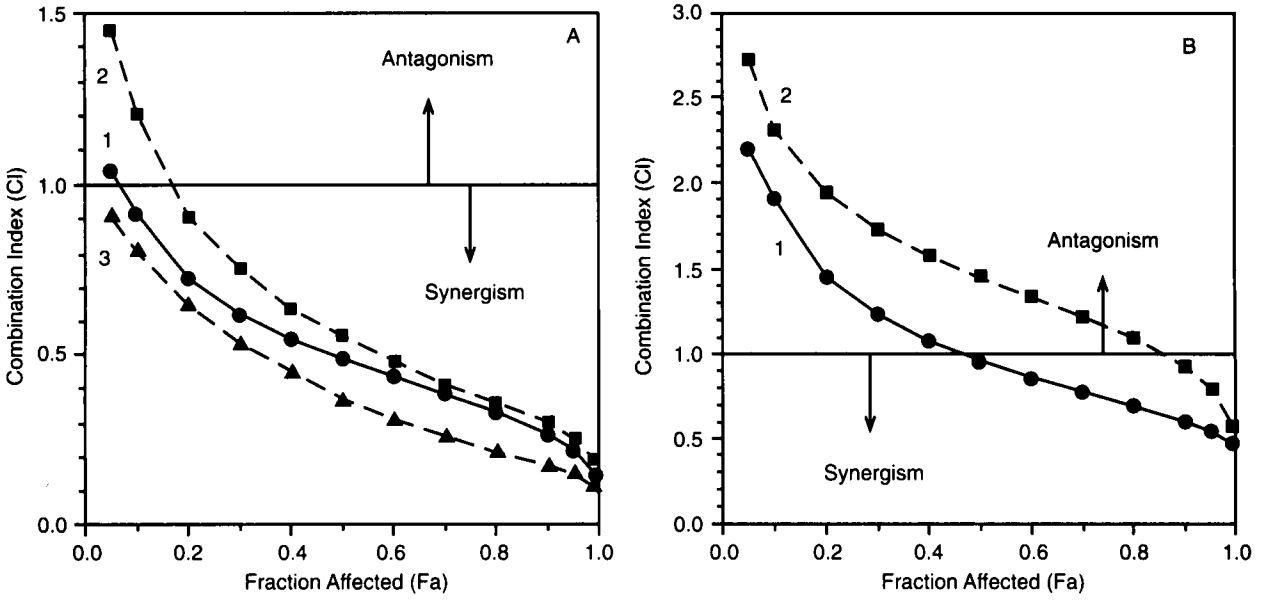

Figure 3. (A) Combination index (CI) plots obtained after simultaneous treatment of cells with VP-16 for 20 min and pre-incubated before photosensitization with $AlPcS_4$ for 4 h; light dose 7.2 J/cm^2 (1, ●) and $ZnPcS_4$ for 4 h; light dose 7.2 J/cm^2 (2, ■), or 9.0 J/cm^2 (3, ▲). Drugs molar ratio: [VP-16]/[$MePcS_4$] = 1/2. (B) Combination index plots when VP-16 treatment was applied after pre-incubation of cells with $AlPcS_4$ (1, ●) or $ZnPcS_4$ (2, ■) for 24 h followed by exposure to 7.2 J/cm^2 red light. Drugs molar ratio: [VP-16]/[$MePcS_4$] = 1/1.

DNA strand breaks induced by single and combined drug treatments

VP-16 was able to damage DNA in K562 cells by inducing a rapid (following a 5–10 min incubation) formation of both 'protein-linked' and 'frank' DNA strand breaks, as revealed by alkaline elution experiments performed in the presence or absence of proteinase K. The ratio of protein-linked and frank breaks varied slightly with the incubation time of the drug with the cells, but in general was close to 1:1. The variation in the number of DNA breaks after incubation of cells with different VP-16 concentrations for 20 min is shown in Figure 4(A). The total DNA breaks formed after combined treatment with VP-16 and photosensitization in the presence of $AlPcS_4$ or $ZnPcS_4$ are also shown in the same figure. The combined treatments produced a supra-additive number of DNA strand breaks as compared with individual drug action, although the number of strand breaks was not linear with respect to VP-16 concentrations. Under these conditions (see legend), and in contrast to the case of $AlPcS_4$, photosensitization with $ZnPcS_4$ did induce DNA breaks by itself. In the absence of VP-16 and after longer pre-irradiation incubation times (24 h or more) of photosensitizers with cells, both the $AlMePcS_4$ and $ZnMePcS_4$ induced relatively high levels of strand breaks and supra-additivity during combination treatment was less pronounced, or even absent (not shown). We also found that longer incubations of cells with VP-16 (30–40 min) tended to reduce the supra-additive formation of DNA strand breaks.

Over a wide range of concentrations, the K562 cells exposed to BSO alone did not reveal any detectable DNA breakage. However, treatment of cells with BSO followed by exposure to etoposide for 20 min resulted in a supra-additive increase in the number of DNA strand breaks, as compared with the action of VP-16 alone (Figure 4B). Although toxic concentrations of BSO (greater than 200 μM) did not induce DNA breaks, the effect of supra-additivity after combined treatment tended to decrease with increasing BSO concentration (up to 2 mM) (not shown).

Correlation between depletion of cytoplasmic GSH and the rate of quenching of the VP-16 phenoxyl radical

Glutathione content (GSH) in K562 cytoplasmic lysates was estimated to be 12.6 ± 0.9 nmol/10^6 cells. Incubation of cells with different concentrations of BSO resulted in a gradual decrease in

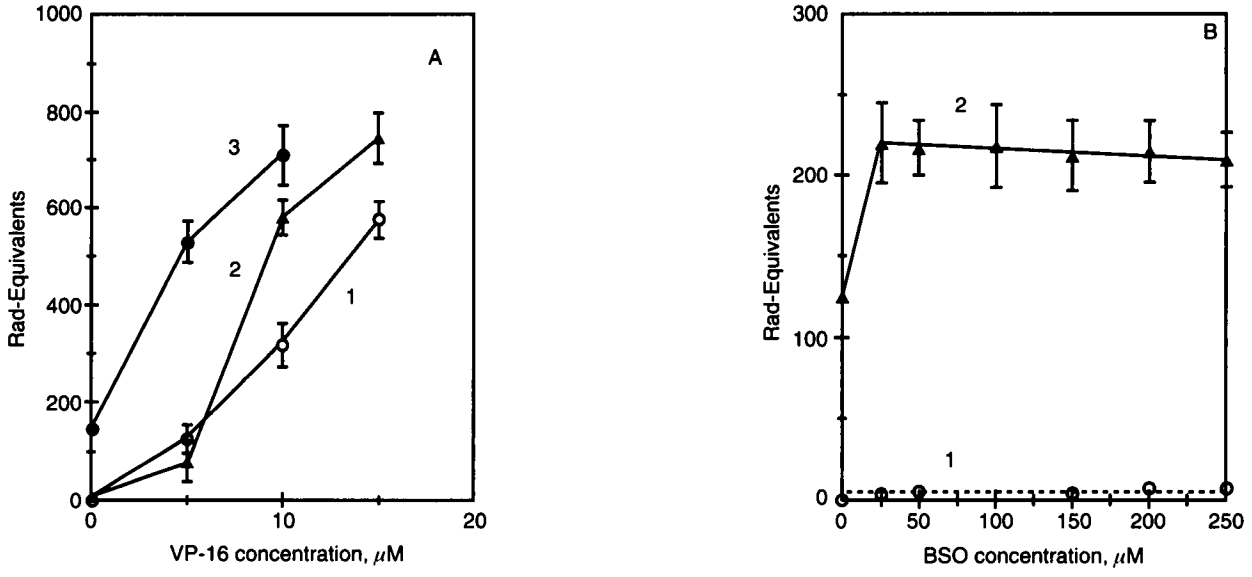

Figure 4. Induction of DNA breaks by individual and combined drug treatment. (A) DNA breaks after incubation of cells with different VP-16 concentrations alone for 20 min (1, ○) and after combined treatment with $AlPcS_4$ (40 μM; 4 h) (2, ▲) or with $ZnPcS_4$ (40 μM; 4 h) (3, ●). Light dose 9 J/cm^2. (B) Effect of pre-incubation of cells with different concentrations of BSO for 4.5 h on the level of VP-16-induced DNA single-strand breaks: BSO alone (1, ○) and in combination with VP-16 (5 μM for 20 min) (2, ▲). Average data from triplicate experiments.

glutathione concentration (Figure 5). GSH content was diminished to about 50% after treatment with 200 μM BSO for 4.5 h. Photosensitization of cells pre-incubated in the dark with $AlPcS_4$ and exposed to various doses of red light also resulted in a dramatic decrease in GSH levels in cell cytoplasm (Figure 5). Under the described conditions, cytoplasmic GSH was decreased to 50% after application of a light dose of about 7.5–8.0 J/cm^2. Similar results for GSH depletion were obtained using $ZnPcS_4$, although the light dose efficiency, as compared to $AlPcS_4$, was lower (Figure 5).

Metabolic transformations of VP-16 to ultimate quinoid products is proceeded by the formation of its phenoxyl radical.[28] We focused out attention on the correlation between the levels of cytoplasmic GSH content and the rate of generation of VP-16 phenoxyl radicals by exogenously added tyrosinase in cytoplasmic preparations. Tyrosinase catalyses the generation of VP-16 phenoxyl radicals with typical ESR parameters for this intermediate (Figure 6, insert) and the steady-state levels of radical concentration in buffer are reached within 4–5 min after mixing the reagents. The presence of reducing compounds, capable of donating electrons to the phenoxyl radical (e.g. GSH) results in a lag period before the ESR signal appearance. During this lag period reductants are consumed and the persistence

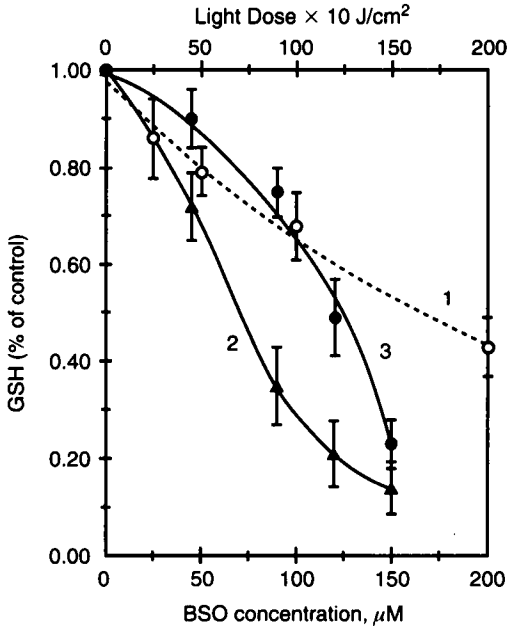

Figure 5. Dependence of GSH depletion on BSO concentration after incubation with cells for 4.5 h (1, ○) (bottom *x*-axis) and photodynamic depletion induced by $AlPcS_4$ (2, ▲) or $ZnPcS_4$ (3, ●) photosensitization following different light doses (upper *x*-axis). $MePcS_4$ (40 μM) was pre-incubated with cells for 4 h. Data points represent mean values from at least five determinations ± SD. Initial GSH content in cytoplasm was 12.6± 0.9 nmol/10^6 cells.

of the lag period is proportional to the concentration of antioxidants in medium.[14] Figure 6 shows typical time-courses of the emergence of the ESR signal of the phenoxyl radical when the reaction was performed in the cytoplasm from untreated cells (curve 1) and in samples where cells were photosensitized in the presence of $AlPcS_4$ with different light doses prior to the isolation of cytoplasm (curves 2–4). A similar shortening of the lag periods was observed when cells were pre-treated with different concentrations of BSO which paralleled the depletion of cytoplasmic GSH (Figure 5). We next studied the effects of thiol reagents (GSH peroxidase/cumene hydroperoxide, or 2-vinylpyridine) on the time of appearance of the ESR signal of the phenoxyl radical and the rates were correlated with the measured amount of reduced GSH in cytoplasm. These results, together with the data obtained from samples subjected to photosensitization and BSO induced depletion of GSH, are summarized in Figure 7. Based on linear regression analysis, we estimated that the prolongation of the lag period before the appearance of the phenoxyl radical ESR signal and the content of reduced GSH in cytoplasm are highly correlated ($r^2 = 0.975$). This result indicates that cytoplasmic levels of GSH can be of crucial importance for intracellular metabolic transformation of VP-16.

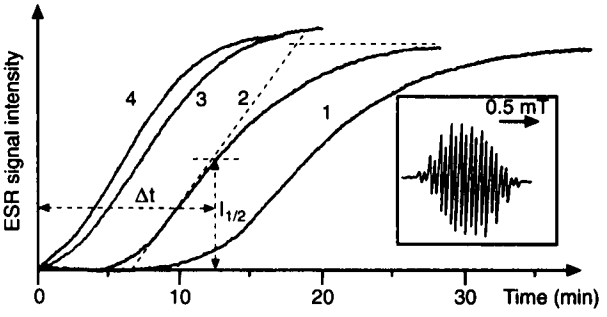

Figure 6. Kinetics of the appearance of the ESR signal of VP-16 phenoxyl radical generated by tyrosinase in cytoplasm isolated from 2×10^6 cells. Untreated cells (line 1) and after cell photosensitization with $AlPcS_4$ applying light doses of: 4, 8 and 15 J/cm^2 (lines 2, 3 and 4). Insert: ESR spectrum of VP-16 phenoxyl radical generated by tyrosinase (5 U/μl) in buffer: $6a_H$ (OCH_3) = 0.131 mT; $2a_H$ (phenoxy) = 0.130 mT; $a_H(\beta) = 0.40$ mT and $a_\gamma = 0.06$ mT).

Discussion

Effects of GSH depletion by BSO on VP-16 toxicity

Early indications of a possible involvement of GSH in VP-16 toxicity were derived from the increased GSSG content and decreased levels of GSH in mouse liver after administration of VP-16.[29] Subsequently, it was shown that GSH can react directly with the *ortho*-quinone derivative and its semi-quinone free radical, interactions capable of protecting DNA from inactivation *in vitro*.[30] In both cases, metabolic transformations of VP-16 are obviously a prerequisite for the reaction with GSH. More recent studies have revealed the importance not only of GSH, but also other antioxidants (e.g. ascorbic acid and protein-bound thiols) in the modulation of etoposide cytotoxicity.[12,17] A new type of interaction has been shown to occur during the initial step of enzymatic (e.g. by several peroxidases and tyrosinase) oxidation of VP-16 when the phenoxyl radical of the drug is formed: one-electron quenching of the radical (reduction to the original etoposide structure),

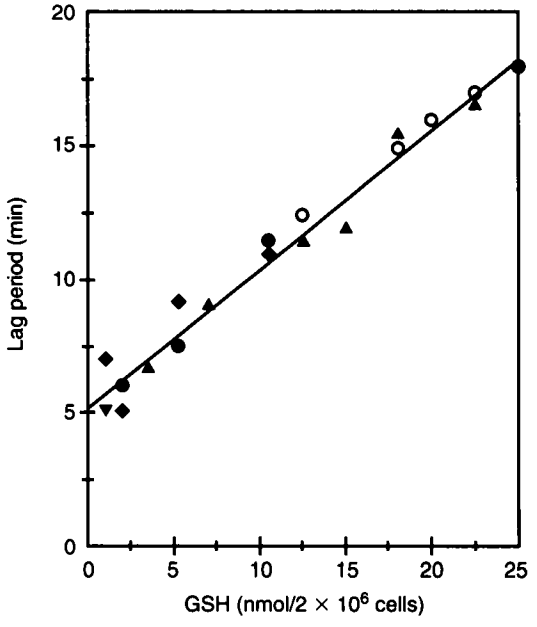

Figure 7. Relationships between GSH content and the lag period (Δt, Figure 6) for the appearance of the VP-16 phenoxyl radical ESR signal in cell cytoplasm after photodynamic treatment with cells preincubated with 40 μM $AlPcS_4$ (●) and $ZnPcS_4$ (▲) and irradiated with light doses from 2.5 to 20 J/cm^2 or exposed to BSO concentrations from 25 to 200 μM (○). Data points (▼) and (◆) represent results obtained after exposure of cell cytoplasm to GSH-px (2 U/μl)/CumOOH (300 μM) or to different concentrations of 2-vinylpyridine, respectively. The line is a result of linear regression fit of all data points (r^2=0.975).

accompanied by a depletion of the pool of cellular antioxidants and, eventually, by generation of superoxide ions.[14,18]

The combination index analysis, as performed in the present study, unequivocally shows that low-to-moderate GSH depletion (below about 50%) by BSO potentates VP-16 cytotoxicity (Figure 2). Similarly, our results indicate a 2-fold increase in the level of DNA breaks when VP-16 was applied together with a wide range of non-toxic BSO concentrations (Figure 4B). In a previous study, the increased VP-16 toxicity after GSH depletion in the presence of BSO was linked to a decreased efflux of the drug and, respectively, increased intracellular concentrations.[31] To observe this effect, however, a minimum time of at least 24 h of BSO pre-incubation (GSH depletion) was required. In the present study we employed short incubation times with VP-16 (20 min) and BSO (4.5 h) to avoid secondary effects of GSH depletion on cell metabolism, as well as to minimize the toxicity of the individual drugs. We, therefore, expect that under our experimental conditions VP-16 accumulation in cells was unaffected by BSO and that the cellular responses to GSH depletion resulted from decreased protection against cytotoxic VP-16 metabolites. This conclusion is supported by the VP-16 phenoxyl radical quenching experiments (Figures 6 and 7). Furthermore, if pre-incubation with higher doses of BSO did affect VP-16 retention in cells, we should have observed stronger ('pseudo') synergism when the cells were highly damaged. In fact, the graphs in Figure 2 show the opposite tendency of additivity (mutually exclusive) and/or antagonism (non-exclusive interactions) in the region when $F_a \rightarrow 1.0$. We suggest that the decreased synergism is related to the more pronounced BSO toxicity when higher (greater than 180 μM) concentrations were applied.

Combination toxicity between VP-16 and photosensitization

When relatively short pre-illumination incubation times with $MePcS_4$ were used the combination index analysis predicted largely synergistic cytotoxic interactions between VP-16 and $AlPcS_4$ or $ZnPcS_4$ photosensitization. The overall synergy with $AlPcS_4$ along the entire F_a range was somewhat higher and was achieved using lower light dose, as compared to $ZnPcS_4$ (Figure 3A). This effect paralleled the higher rate of GSH depletion after photosensitization in the presence of $AlPcS_4$ (Figure 5). Similarly, we have previously found that $ZnPcS_4$ has a lower oxidative efficiency against other thiols and for the photoinactivation of intracellular catalase,[23] although usually in *in vitro* experiments this compound exhibits higher cytotoxicity than $AlPcS_4$.[22,32] Both photosensitizers possess similar triplet state quantum yields when in monomeric form, but $ZnPcS_4$ has a greater tendency to dimerize or aggregate, which is known to decrease the efficiency of generation of activated oxygen species (singlet oxygen and free radicals) after photo-excitation. It is also likely that photosensitized oxidation in GSH might be not a primary intracellular target, especially for $ZnPcS_4$, as seen from the initial lag in GSH depletion with respect to the applied light dose (Figure 5) and from the ability of this photosensitizer to induce DNA strand breaks in the absence of VP-16 (Figure 4A). The combination treatment of cells with relatively low concentrations of VP-16 and photosensitization resulted in a synergistic increase of the level of DNA breaks (Figure 4A). When the dyes were incubated for a longer time before irradiation their individual toxicity changed enormously [e.g. for $AlPcS_4$ IC_{50} changed from about 32 ± 4 μM (4 h) to 3.4 ± 0.8 μM (24 h), at constant VP-16 $IC_{50} = 9.5 \pm 0.8$ μM (20 min)]. We consider this dramatic change in photodynamic toxicity to be the result of a different intracellular localization of $MePcS_4$ and the targeting of specific molecular structures (including DNA).[33] This might be the reason for the higher antagonism revealed by combination index analysis under such conditions, as well (Figure 3B). In all cases, as higher light doses or concentrations were applied the antagonistic interactions were converted to synergistic (Figure 3A and B). One attractive hypothesis to explain these results comes from earlier[34] and recent[35] observations that anionic phthalocyanines are primarily localized in lysosomes (in the dark) and after initial photo-irradiation are released into the cytoplasm or re-localize in other organelles. Due to these events, following an increase in light dose the efficiency of photosensitized oxidation of cytoplasmic GSH would obviously be higher.

Based on our previous experiments,[23] we consider that $MePcS_4$ photosensitization and the generated active oxygen forms are primarily responsible for the direct oxidation of GSH. However, in cells the GSH–peroxidase cycle may also be involved in the process of depletion of GSH after irradiation, since photosensitization is expected to produce various peroxides as substrates. Further studies are required to quantify the relative importance of each pathway of GSH depletion during photosensitization.

As demonstrated in this study, depletion of GSH in the cytoplasm by different treatments results in a

more effective accumulation of the VP-16 phenoxyl radical, which allows further metabolic or oxidative transformations of the drug. The strong correlation between the lag period during which the phenoxyl radical is continuously converted back to the original form of the drug and the cytoplasmic level of GSH (Figure 7) definitively suggests that glutathione content is important for the effectiveness of VP-16 intracellular redox-transformations and consequently for etoposide cytotoxicity. For example, VP-16 is about 10 times more toxic in HL60 human leukemic cells than it is in K562 cells.[36] Interestingly, the GSH content of HL60 cells was reported to be in the range of 1.1 nmol/10^6 cells,[37] which is approximately 10% of the GSH content in K562 cells. As demonstrated by Usui and Sinha[10] who used two melanoma cell lines with different tyrosinase activities, the intracellular levels of VP-16 metabolizing enzymes would also be expected to be of crucial importance in modulating drug toxicity.

Conclusion

In this study we have shown that enzymatic and photodynamic depletion of GSH, which provides a specific thiol-dependent type of oxidative stress, enhances VP-16 cytotoxic activity. Since etoposide is often utilized as a component in combination chemotherapy, we anticipate that further understanding of its redox transformations, and particularly its interactions with oxidtive stress-related cancer treatment modalities (e.g. PDT), may provide new perspectives for clinical applications.

Acknowledgments

The authors are grateful to Dr JE van Lier for the gift of phthalocyanines and to Ms B Gowans for her technical assistance.

References

1. Liu LF. DNA topoisomerase poisons as antitumour drugs. *Annu Rev Biochem* 1989; **58**: 351–75.
2. van Maanen JMS, Lafleur MVM, Mans DRA, *et al.* Effects of the *ortho*-quinone and catechol of the antitumor drug VP-16-213 on the biological activity of single-stranded and double-stranded ΦX174 DNA. *Biochem Pharmacol* 1988; **37**: 3579–89.
3. Wozniak AJ, Ross WE. DNA damage as a basis for 4′-demethylepipodophyllotoxin-9-(4,6-*O*-ethylidene-β-D-glucopyranoside) (Etoposide) cytotoxicity. *Cancer Res* 1983; **43**: 120–4.
4. Loike JD, Horwitz SB. Effect of VP-16-213 on the intracellular degradation of DNA in HeLa cells. *Biochemistry* 1976; **15**: 5443–8.
5. Haim N, Roman J, Nemec J, Sinha BK. Peroxidative free radical formation and *O*-demethylation of etoposide (VP-16) and teniposide (VM-26). *Biochem Biophys Res Commun* 1986; **135**: 215–20.
6. Mans DRA, Retèl J, van Maanen JMS, *et al.* Role of the semi-quinone free radical of the anti-tumour agent etoposide (VP-16-213) in the activation of single- and double-stranded ΦX174 DNA. *Br J Cancer* 1990; **62**: 54–60.
7. Mans DRA, Lafleur MVM, Westmijze EJ, *et al.* Formation of different reaction products with single- and double-stranded DNA by the *ortho*-quinone and the semi-quinone free radical of etoposide (VP-16-213). *Biochem Pharmacol* 1991; **42**: 2131–2139.
8. van Maanen JMS, de Vries J, Pappie D, *et al.* Cytochrome P-450-mediated *O*-demethylation: a route in the metabolic activation of etoposide (VP-16-213). *Cancer Res* 1987; **47**: 4658–62.
9. Haim N, Nemec J, Roman J, Sinha BK. Peroxidase-catalyzed metabolism of etoposide (VP-16-213) and covalent binding of reactive intermediates to cellular macromolecules. *Cancer Res* 1987; **47**: 5835–40.
10. Usui N, Sinha BK. Tyrosinase-induced free radical formation from VP-16-213: relationship to cytotoxicity. *Free Radical Res Commun* 1990; **10**: 287–93.
11. Sinha BK, Antholine WM, Kalyanaraman B, Eliot HM Copper ion-dependent oxyradical mediated DNA damage from dihydroxy derivative of etoposide. *Biochim Biophys Acta* 1990; **1096**: 81–3.
12. Goldman R, Stoyanovsky DA, Day BW, Kagan VE. Reduction of phenoxyl radicals by thioredoxin results in selective oxidation of its SH-groups to disulfides. An antioxidant function of thioredoxin. *Biochemistry* 1995; **34**: 4765–72.
13. Ritov VB, Goldman R, Stoyanovsky DA, Menshikova EV, Kagan VE. Antioxidant paradoxes of phenolic compounds: Peroxyl radical scavenger and lipid antioxidant, etoposide (VP-16), inhibits sarcoplasmic reticulum Ca^{2+}-ATPase via thiol oxidation by its phenoxyl radical. *Arch Biochem Biophys* 1995; **321**: 140–52.
14. Gantchev TG, van Lier JE, Stoyanovsky DA, Yalowich JC, Kagan VE. Interactions of phenoxyl radical of antitumor drug, etoposide, with reductants in solution and in cell and nuclear homogenates: electron spin resonance and high-performance liquid chromatography. *Methods Enzymol* 1994; **234**: 631–42.
15. Yokomizo A, Ono M, Nanri H, *et al.* Cellular levels of thioredoxin associated with drug sensitivity to cisplatin, mitomycin C, doxorubicin, and etoposide. *Cancer Res* 1995; **55**: 4293–6.
16. Tyurina YY, Tyurin VA, Yalowich JC, *et al.* Phenoxyl radicals of etoposide (VP-16) can directly oxidize intracellular thiols: protective versus damaging effects of phenolic antioxidants. *Toxicol Appl Pharmacol* 1995; **131**: 277–88.
17. Kagan VE, Yalowich JC, Day BW, Goldman R, Gantchev TG, Stoyanovsky DA. Ascorbate is the primary reductant of the phenoxyl radical of etoposide in the presence of thiols both in cell homogenates and in model systems. *Biochemistry* 1994; **33**: 9651–60.
18. Stoyanovsky DA, Goldman R, Claycamp HG, Kagan

VE. Phenoxyl radical-induced thiol-dependent generation of reactive oxygen species: implications for benzene toxicity. *Arch Biochem Biophys* 1995; **317**: 315–23.
19. Orrenius S, Moldeus P. The multiple role of glutathione in drug metabolism. *Trends Pharmacol Sci* 1984; **5**: 423–35.
20. Bump EA, Yu NY, Brown JM. Radiosensitization of hypoxic tumor cells by depletion of intracellular glutathione. *Science* 1982; **217**: 544–5.
21. Meister A, Griffith OW. Effects of methionine sulfoximine analogs on synthesis of glutamine and glutathione: possible chemotherapeutic implications. *Cancer Treat Rep* 1979; **63**: 1115–21.
22. Gantchev TG, Brasseur N, van Lier JE. Combination toxicity of etoposide (VP-16) and photosensitisation with a water-soluble aluminium phthalocyanine in K562 human leukaemic cells. *Br J Cancer* 1996; **74**: 1570–7.
23. Gantchev TG, van Lier JE. Catalase inactivation following photosensitization with tetrasulfonated metallophthalocyanines. *Photochem Photobiol* 1995; **62**: 123–34.
24. Chou TC, Talalay P. Quantitative analysis of dose–effect relationships: the combined effects of multiple drugs or enzyme inhibitors. *Adv Enzyme Reg* 1983; **22**: 27–55.
25. Kohn KW, Erickson LC, Ewig RAG, Friedman CA. Fractionation of DNA from mammalian cells by alkaline elution. *Biochemistry* 1976; **15**: 4629–37.
26. Hunting DJ, Gowans BJ. Inhibition of repair patch ligation by an inhibitor of Poly(ADP-ribose) synthesis in normal human fibroblasts damaged with ultraviolet radiation. *Mol Pharmacol* 1987; **33**: 358–62.
27. Griffith OW. Determination of glutathione and glutathione disulfide using glutathione reductase and 2-vinylpyridine. *Anal Biochem* 1980; **106**: 207–12.
28. Kalyanaraman B, Nemec J, Sinha BK. Characterization of free radicals produced during oxidation of etoposide (VP-16) and its catechol and quinone derivatives. An ESR study. *Biochemistry* 1989; **28**: 4839–46.
29. Katki AG, Kalyanaraman B, Sinha BK. Interactions of the antitumor drug, etoposide, with reduced thiols *in vitro* and *in vivo*. *Chem-Biol Interact* 1987; **62**: 237–47.
30. Mans DRA, Lafleur MVM, Westmijze EJ, *et al.* Reactions of glutathione with the catechol, the *ortho*-quinone and the semi-quinone free radical of etoposide. *Biochem Pharmacol* 1992; **43**: 1761–8.
31. Mans DRA, Schuurhuis GJ, Treskes M, *et al.* Modulation by D,L-buthionine-*S*,*R*-sulphoximine of etoposide cytotoxicity on human non-small cell lung, ovarian and breast carcinoma cell lines. *Eur J Cancer* 1992; **28A**: 1447–52.
32. Gantchev TG, Urumov IJ, Hunting DJ, van Lier JE. Photocytotoxicity and intracellular generation of free radicals by tetrasulphonated Al- and Zn-phthalocyanines. *Int J Radiat Biol* 1994; **65**: 289–98.
33. Hunting DJ, Gowans BJ, Brasseur N, van Lier JE. DNA damage and repair following treatment of V-79 cells with sulfonated phthalocyanines. *Photochem Photobiol* 1987; **45**: 769–73.
34. Peng Q, Farrants GW, Madslien K, *et al.* Subcellular localization, redistribution and photobleaching of sulfonated aluminum phthalocyanines in a human melanoma cell line. *Int J Cancer* 1991; **49**: 290–5.
35. Wood SR, Holroyd JA, Brown SB. The sub-cellular localization of Zn(II)phthalocyanines and their redistribution on exposure to light. *Photochem Photobiol* 1996; **63S**; SPM-F4.
36. Dubrez L, Goldwasser F, Genne P, Pommier Y, Solary E. The role of cell cycle regulation and apoptosis triggering in determining the sensitivity of leukemic cells to topoisomerase I and II inhibitors. *Leukemia* 1995; **9**: 1013–24.
37. Raghu G, Pierre-Jerome M, Dordal MS, Simonian P, Bauer KD, Winter JN. P-glycoprotein and alterations in the glutathione/glutathione-peroxidase cycle underlie doxorubicin resistance in HL-60-R, a subclone of the HL-60 human leukemia cell line. *Int J Cancer* 1993; **53**: 804–11.

(Received 19 November 1996; accepted 26 November 1996)